Journal of Mechanical Science and Technology 24 (2010) 415~420
www.springerlink.com/content/1738-494x
DOI 10.1007/s12206-009-1112-y

Behavior of thermal bubbles formed from a single nucleation site†

Young Soo Chang[1], Kwang-Hun Jeong[2], Heon Ju Lee[1], Yoon Pyo Lee[1] and Ho-Young Kim[2,*]
[1]*Energy Mechanics Research Center, Korea Institute of Science and Technology, Seoul 136-791, Korea*
[2]*School of Mechanical and Aerospace Engineering, Seoul National University, Seoul 151-744, Korea*

(Manuscript Received March 4, 2009; Revised September 27, 2009; Accepted September 27, 2009)

Abstract

Thermal bubble formation is a fundamental process in nucleate boiling heat transfer and in many microelectromechanical thermal systems. Here, we report an experimental study of the dynamic and thermal behavior of bubbles generated at a single site, that is, a microcavity filled with alumina particles. The thermal process associated with the bubble departure from the isolated cavity, in particular, was shown to be different from that of macroscale boiling. The bubble departure diameter remains constant in a low superheat (or Jakob number) regime which is solely determined by the balance of interfacial tension and buoyancy. In addition, the bubble departure frequency increases along the bubble size as the substrate temperature rises. The further-increased frequency of bubbles emerging from the cavity causes multiple bubbles to coalesce before the preceding bubble completely detaches from the substrate, thus, leading to the decrease of apparent departure frequency with the increase of substrate temperature.

Keywords: Thermal bubble; Microcavity; Boiling; MEMS

1. Introduction

The behavior of thermal bubbles generated by the boiling of liquids has been the subject of intense study for decades [1-4]. In addition to the conventional industrial applications associated with boiling, thermal bubbles have been successfully utilized in ink-jet printing technology [5]. Recent novel applications of thermal bubbles, including cooling of electronic devices, microactuation [6], micropump/mixer [7, 8], and biosample delivery [9], have drawn renewed interest in this area. The boiling phenomena in microthermal systems, especially, require an understanding of individual bubble behavior, for which conventional approaches of investigating collective behavior of bubbles are often inadequate.

Recently, a novel heat engine utilizing a thermal bubble was reported [10]. Thermal energy supplied to the liquid generates a bubble, which grows to deflect a flexible solid cantilever situated adjacent to a single nucleation site. A continuous supply of heat leads to the repetitive generation of bubbles, and thus, a periodic motion of the cantilever beam that can be considered dc (direct current) to ac (alternating current) conversion. One can construct a microscale electric power generation system using this scheme by coating the cantilever with a lead zirconate titanate (PZT) film that converts mechanical stress to electrical charge [11]. To realize this microscale power generation system, it is essential to generate thermal bubbles at a designated site with a substantially low superheat.

Microheaters that were fabricated using microfabrication technology were frequently used to generate a single thermal bubble [12-14]. These studies found that a significant amount of superheat is necessary to form a bubble on smooth surfaces of such materials as polysilicon and platinum. It is attributed to the absence of cavities on solid surfaces, which are known

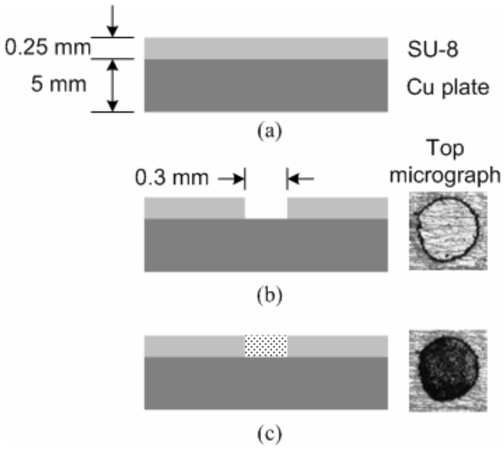

Fig. 1. Fabrication process flow of porous microcavity: (a) Spin-coating of SU-8 on a copper plate. (b) Developing a cylindrical hole on the photoresist. (c) Injection of microparticles into the hole.

---

† This paper was recommended for publication in revised form by Associate Editor Dongsik Kim

*Corresponding author. Tel.: +82 2 880 9286, Fax.: +82 2 880 9287
E-mail address: hyk@snu.ac.kr

to facilitate bubble nucleation owing to unsaturated, trapped gas within. Compared to the individual bubbles nucleated on microfabricated line or film heaters, the behavior of individual thermal bubbles generated at a single nucleation site on a macroscopically heated surface (e.g., copper surfaces heated by cartridge heating blocks) has been less intensively investigated experimentally. Siegel and Keshock [15] used a smooth solid surface with a few nucleation sites in a reduced gravity condition to measure the growth rate and departure frequency of the bubbles generated from a single spot. The interests of their work were centered on the effect of reduced gravity, thus the effects of thermal conditions (e.g. temperature and pressure) on the behavior of bubbles were not addressed. Son, Dhir, and Ramanujapau [16] artificially formed a microcavity on a silicon wafer to nucleate a single bubble. Their work was focused on verifying their numerical model with the experimental data (bubble growth rate), not on the effects of varying thermal conditions on bubble behavior.

Therefore, this study aims to provide novel experimental findings of the nucleate boiling behavior at a single nucleation site on a surface that is heated macroscopically. In particular, we report how the departure diameter and frequency of bubbles generated at a single spot depend on the ambient pressure and heating surface temperature. We show that such behavior of bubbles from a single nucleation site is qualitatively different from that of bubbles on normal surfaces with abundant nucleation sites.

We describe a novel method to generate a single bubble with a very low superheat from a cavity filled with microparticles. It was previously reported that a porous coating of solid surfaces significantly reduced the superheat for bubble incipience [17]. However, we combine this method with photolithography technology to generate a thermal bubble at a designated site with a substantially low superheat. We also investigate various thermal behavior of bubbles formed from this isolated nucleation site to find the differences of the behavior of the bubbles of interest with that of bubbles generally observed in macroscale boiling.

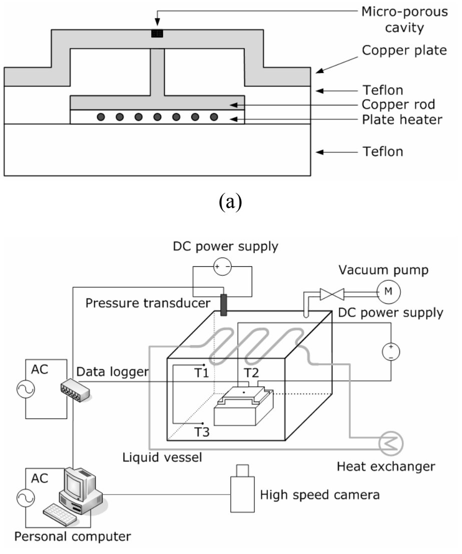

(a)

(b)

Fig. 2. Experimental setup: (a) Schematic cross-section of the bubble generation part, (b) Overall experimental setup including the liquid chamber, the temperature and pressure control systems, and the imaging system.

2. Experiments

To generate a thermal bubble at a designated site with reduced superheat, we fabricated a cavity filled with microparticles on a smooth surface using the process shown in Fig. 1. A copper plate was spin-coated with a photoresist, SU-8, up to the final thickness of 250 μm. The photoresist layer was exposed to ultraviolet rays through a photomask and chemically developed to open a microcavity with a diameter of 300 μm and depth of 250 μm. The cavity was filled with a mixture of alumina particles (A), epoxy (E), and isopropyl alcohol (I) with a mass ratio of A:E:I = 2:1:10. The size of alumina particles ranged between 1 and 20 μm. Figure 1 includes the top view of the fabricated cavity before and after the hole was filled with particles.

The copper plate having the particle-filled cavity was joined to a heating block, as illustrated in Fig. 2(a). A copper rod, placed right below the cavity, transmitted heat from a heater to the copper plate to minimize image distortion during optical measurement, which might be caused by the violent natural convection of the surrounding liquid if the entire plate were heated. The cavity consisted of a Cu bottom surface and an SU-8 sidewall, and its temperature was measured by a copper-constant thermocouple embedded in the copper plate 2 mm below the microcavity. We may ignore the temperature gradient between the thermocouple and the cavity considering the insulating nature of the SU-8 film having a low thermal conductivity of 0.2 W/mK. As shown in Fig. 2(b), the overall experimental setup consisted of a chamber that houses liquid and the heating block, a dc power supply to power the heater, a temperature measurement system, and a high-speed camera. The temperature of the liquid was maintained by a heat exchanger that runs water, and the pressure inside the chamber was controlled by a vacuum pump.

The liquid used in the experiments was FC-72, whose saturation temperature (T_s) is 56° C at 1 atm. We used different values of chamber pressure such as 0.32 atm (T_s=26.1° C), 0.38 atm (T_s=30.3° C), 0.47 atm (T_s=35.9° C), and 0.54 atm (T_s=39.6° C). The substrate temperature was varied by controlling a current supplied to the heater while the liquid temperature was maintained at 25° C. The images of thermal bubbles formed at the cavity were recorded by a high-speed CCD camera (Redlake PCI 2000S) running with the rate of 1,000 frames per second.

3. Results and discussions

The minimum superheat ΔT_n triggering the bubble nu-

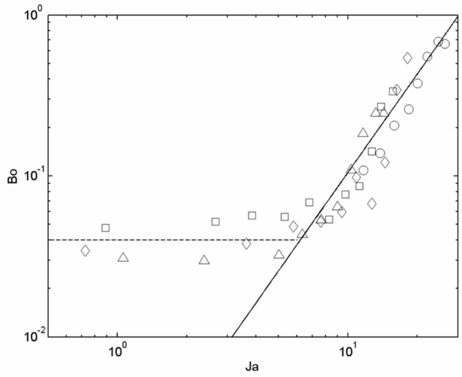

Fig. 3. The effect of the superheat (*Ja*) on the departure diameter (*Bo*) for the bubbles nucleated at porous microcavities. The circles, diamonds, squares, and triangles correspond to the pressure of 0.32 atm, 0.38 atm, 0.47 atm, and 0.54 atm, respectively. The solid line is from Eq. (4) with $C_1 = 0.492$ and $C_2 = 0.033$, and the dashed line indicates *Ja*=0.06.

cleation is defined as $\Delta T_n = T_{h,n} - T_s$, where $T_{h,n}$ is the measured cavity temperature at which a thermal bubble first appears. In all pressure conditions, ΔT_n was measured to be as low as 2.6° C, or less, indicating superior performance of the microporous cavity in lowering the minimum superheat. To evaluate the effects of microparticles occupying the hole, we heated a substrate having a microcavity with a diameter of 300 μm and no inner microparticles, to find no bubble formation even until the superheat reached 10° C in the same pressure range as above. A similar finding was reported by Qi and Klausner [18], where no bubble was formed when the superheat reached 20° C because the liquid completely filled the cylindrical hole.

The departure diameter, that is, the bubble diameter just released from a solid surface, is dependent on various thermophysical properties of the liquid and the superheat. The relationship has been frequently given by correlating to the Bond number.

For instance, Eq. (1) is used to calculate a response surface as follows:

$$Bo = \frac{(\rho_l - \rho_v) g d^2}{\sigma} \tag{1}$$

with the Jakob number,

$$Ja = \frac{\rho_l c_l (T_w - T_s)}{\rho_v h_{fg}} \tag{2}$$

where ρ_l and ρ_v are the densities of liquid and vapor, respectively, *d* is the departure diameter, *g* is the gravitational acceleration, σ is the surface tension, c_l is the specific heat of liquid, T_w is the wall temperature, and h_{fg} is the latent heat of vaporization. Although various correlations were suggested [4], none seem to be universally valid as each study considered different superheat ranges and boiling regimes. We employed the correlation based on Cole [19] to compare with the experimental results:

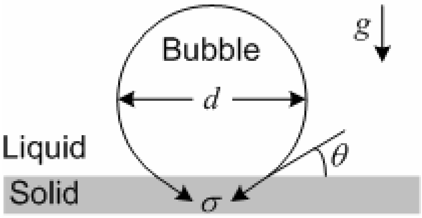

Fig. 4. Bubble configuration before departure.

$$Bo^{C_1} = C_2 Ja \tag{3}$$

where constants C_1 and C_2 were proposed to be 0.5 and 0.04 by Cole [19]. As Fig. 3 shows, the correlation agrees reasonably with the experimental results for the Jakob numbers greater than approximately 6. Here, the values of the constants that best fit the measurement data were determined to be $C_1 = 0.492$ and $C_2 = 0.033$, not far from Cole's values. However, for smaller *Ja*, *Bo* tends to vary only slightly, despite the change of *Ja*. That is, the departure diameters are almost constant in the low superheat range. Therefore, our experiments suggest that when thermal bubbles are formed at a single nucleation site, *Bo* based on the departure diameter is 0.04 for $Ja < 6$ and that Eq. (3) holds for $Ja > 6$:

$$\begin{aligned} &Bo = 0.04 \quad \text{for} \quad Ja < 6 \\ &Bo^{0.492} = 0.033 Ja \quad \text{for} \quad Ja > 6 \end{aligned} \tag{4}$$

The constant Bond numbers of departing bubbles for small *Ja* indicate that in the low superheat conditions, the force balance between the interfacial tension and the buoyancy plays a dominant role in bubble departure rather than other thermal processes, such as convection, which become crucial at high *Ja* ranges. The force balance between the interfacial tension and the buoyancy (see Fig. 4) can be written as

$$\pi d_c \sigma \sin\theta = \frac{\pi}{6} d^3 (\rho_l - \rho_v) g \tag{5}$$

where d_c is the contact diameter of the bubble with the solid and θ the contact angle. For low *Bo*, the bubble assumes a spherical shape, thus, $d_c = d \sin\theta$. Using $Bo = 0.04$, θ is obtained to be 9.4°, which is a reasonable value for FC-72 that has very low contact angles on most solid surfaces.

The bubble departure frequency *f* is defined as the number of bubbles leaving the surface per unit time. It was proposed by previous researchers that the product, $f^n d$, is a constant and that the value of the exponent *n* depends on the bubble growth condition. Ivey [20] argued that $n = 2$ for inertia-controlled growth and $n = 1/2$ for heat-transfer-controlled growth. McFadden and Grassmann [21] and Frederking and Daniels [22] obtained $n = 1/2$ based on their experiments, and Cole [19] experimentally found $n = 1$. Although the val-

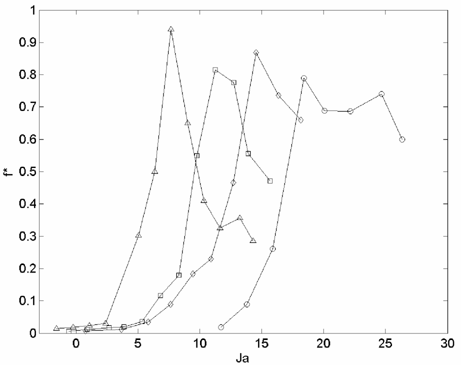

Fig. 5. Dimensionless departure frequency versus the Jakob number. The frequency initially increases but suddenly drops at high Ja due to bubble coalescence. The circles, diamonds, squares, and triangles correspond to the pressure of 0.32 atm, 0.38 atm, 0.47 atm, and 0.54 atm, respectively.

ues of *n* are different, the foregoing works on macroscale boiling commonly showed that *f* decreases as *d* increases. Since *d* increases with the superheat, as shown above, *f* should decrease as the superheat increases according to the previous theories. However, Fig. 5 shows that, in our experiments, the dimensionless frequency f^*, defined in Eq. (6) as

$$f^* = \frac{f(\rho_l^2\sigma)^{1/4}}{[g(\rho_l - \rho_v)]^{3/4}} \tag{6}$$

increases with the increase of *Ja* (or the superheat) before bubble coalescence occurs. That is, the increase of the substrate temperature leads to the increase of both the bubble diameter and the departure frequency when nucleation takes place from a single cavity. Fig. 5 also shows that for the same *Ja (*e.g., $Ja = 6$), f^* is higher when the ambient pressure is higher, thus indicating that bubbles are more easily generated under higher pressure.

In the macroscale boiling, where bubbles are nucleated at numerous sites on a solid surface, as the substrate temperature rises, the increased amount of heat transfer from the substrate to the liquid occurs by the following mechanisms despite the decrease of departure frequency: (1) the volume of vaporizing liquid increases, which carries away more latent heat, and (2) the number of active nucleation sites increases. However, when only a single cavity is present on a substrate, instead of activating other nucleation sites, we found that the departure frequency, as well as the bubble size, increases to enhance the heat transfer rate. We noted that the simultaneous increase of *d* and *f* with the substrate temperature rise was also observed for thermal bubbles nucleated on continuously powered microline heaters [14]. In that study, it was found that the contact diameter of a growing bubble with the microheater increases faster as the heater temperature increases, causing both the departure diameter and frequency to increase.

As shown in Fig. 5, the departure frequency suddenly drops after initial increase upon *Ja* exceeding certain limits that de-

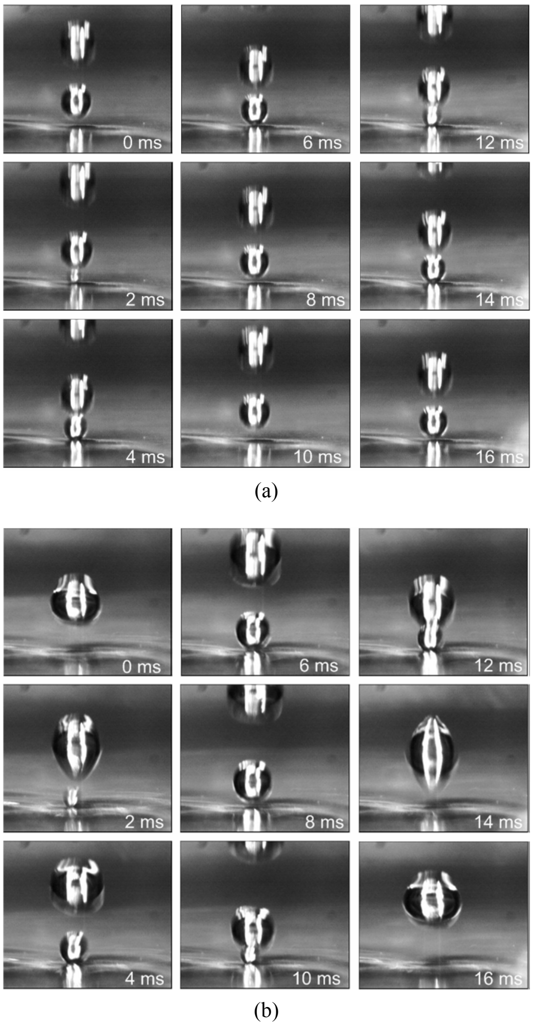

(a)

(b)

Fig. 6. High-speed images of departing bubbles: (a) with the absence of coalescence at the superheat of 3.5° C, and (b) with the coalescence at the superheat of 4.0° C. For both the experiments, the pressure was 0.32 atm.

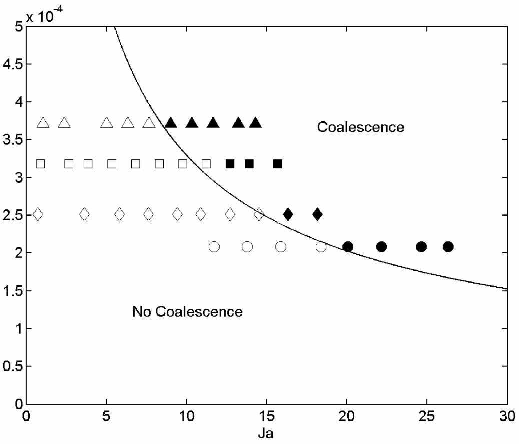

Fig.7. Regime map of bubble coalescence based on P^* and *Ja*. The open symbols indicate experimental conditions under which no coalescence occurs, while the filled ones correspond to the conditions leading to bubble coalescence.

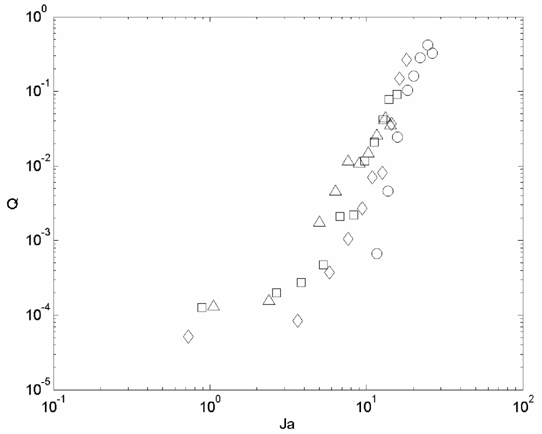

Fig.8. Dimensionless volume of vaporizing liquid per unit time (Q) versus *Ja*. The open symbols indicate experimental conditions under which no coalescence occurs, while the filled ones correspond to the conditions leading to bubble coalescence.

pend on the pressure. This is because the bubbles coalesce while rising from the cavity, as shown in Fig. 6, which compares the bubble departure behaviors with and without the coalescence. The bubble coalescence occurs when the growth rate of a bubble catches up with the rising velocity of a preceding bubble as shown in the image at 14 ms in Fig. 6(b). Also, we observed that the second bubble cannot grow as large as the preceding bubble due to merging in the course of its growth. The resultant bubble vibrates vigorously upon completely disengaging from the surface. Since the coalescence limit is determined not only by the superheat but also by the pressure, we obtained the empirical regime map in the two-dimensional spaces based on the dimensionless superheat *Ja* and the dimensionless pressure P^* , defined as $P^* = P / h_{fg}\rho_l$. Fig. 7 shows that when the *Ja* and P^* of the boiling condition lie above the boundary, whose empirical expression is given by $P^* Ja^{0.7} = 1.65 \times 10^{-3}$, coalescence takes place. Below the boundary, individual bubbles depart from the surface one by one.

Although the bubble coalescence decreases the number of bubbles that carry away thermal energy from the substrate, the volume of the vaporizing fluid does not decrease as *Ja* increases. Fig. 8 plots the dimensionless volume of vaporizing liquid per unit time, Q , versus *Ja*. Here, Q is defined as

$$Q = \frac{fd^3[(g\rho_l^{2/3}(\rho_l - \rho_v)]^{3/4}}{\sigma^{5/4}} \tag{7}$$

following Frederking and Daniels [22]. It shows that as *Ja* increases, the vaporizing volume continuously increases, although the departure frequency drops due to the coalescence for high *Ja*. The increase of the vaporizing volume implies that enhanced heat transfer rate in the form of latent heat is still at work in high *Ja* ranges, which is the essential energy transport mechanism in boiling.

4. Conclusions

We fabricated a porous microcavity using photolithography technology in which a single thermal bubble can be formed with a substantially low superheat. The thermal process associated with the bubble incipience and departure from the isolated cavity is shown to be different from that of macroscale boiling in the following aspects. The bubble departure diameter remains constant in a low *Ja* range (*Ja* < 6), which is solely determined by the balance of interfacial tension and buoyancy. Also, the bubble departure frequency increases along with the bubble size as the substrate temperature rises to enhance the heat transfer rate. The increased frequency of bubbles emerging from the cavity causes multiple bubbles to coalesce before the preceding bubble completely detaches from the substrate, leading to the decrease of apparent departure frequency with the increase of substrate temperature.

The findings obtained in this work can be applied to the design and operation of thermal bubble-based microsystems as well as to the fundamental understanding of the single bubble nucleation boiling process. Furthermore, if the electrical heater utilized in this work is replaced by other external heat sources, such as a computer chip or a human body, and a PZT cantilever beam is located near the microcavity, a microscale power generation system can be realized.

Acknowledgment

The authors are grateful to the Korea Research Council of Fundamental Science and Technology and KIST for their support in this work. One of the authors (H.Y.K.) also acknowledges the support from Woongjin Coway and SNU IAMD.

References

[1] H. K. Forster and N. Zuber, Growth of a vapor bubble in a superheated liquid, *J. Appl. Phys.* 25 (1954) 474-478.

[2] C.-Y. Han and P. Griffith, The mechanism of heat transfer in nucleate boiling – Part I, *Int. J. Heat Mass Transfer* 8 (1965) 887-904.

[3] B. B. Mikic, W. M. Rosehnow and P. Griffith, On bubble growth rates, *Int. J. Heat Mass Transfer* 13 (1970)657-666.

[4] V. P. Carey, *Liquid-Vapor Phase-Change Phenomena, Hemisphere*, Washington, DC. USA (1992).

[5] N. J. Nielsen, History of ThinkJet printhead development, *Hewlett Packard J.* 36 (1985) 4-10.

[6] L. Lin, L., A. P. Pisano and A. Lee, Microbubble powered actuator, *Proc. Int. Conf. Solid-state Sensors and Actuators*, (1991) 1041-1044.

[7] J.-H. Tsai and L. Lin, A thermal bubble actuated micronozzle-diffuser pump, *Proc. IEEE MEMS Workshop* (2001) 409-412.

[8] L. Lin and J.-H. Tsai, Active microfluidic mixer and gas bubble filter driven by thermal bubble micropump, *Sens. Ac-*

tuators A 97/98 (2002) 665-671.

[9] R. B. Maxwell, A. L. Gerhardt, M. Toner, M. L. Gray and M. A. Schmidt, A microbubble-powered bioparticle actuator, *J. Microelectromech. Syst*. 12 (2003) 630-640.

[10] H. J. Lee, Y. S. Chang, Y. P. Lee, K.-H. Jeong and H.-Y. Kim Deflection of microcantilever by growing vapor bubble. *Sens. Actuators A* 136 (2007) 717-722.

[11] H.-Y. Kim, H. J. Lee, Y. S. Chang and Y. P. Lee, Micro power generation based on thermal bubbles, *Proc. 6th KSME-JSME Thermal and Fluids Engineering Conference*, (2005) FK 05.

[12] L. Lin, A. P. Pisano and V. P. Carey, Thermal bubble formation on polysilicon micro resistors, *J. Heat Transfer* 120 (1998) 735-742.

[13] C. T. Avedisian, W. S. Osborne, F. D. McLeod and C. M. Curley, Measuring bubble nucleation temperature on the surface of a rapidly heated thermal ink-jet heater immersed in a pool of water, *Proc. R. Soc. Lond. A* 455 (1999) 3875-3899.

[14] H.-Y. Kim, K.-H. Jeong, S. Ko, H. J. Lee, Y. P. Lee and Y. S. Chang, Life of thermal bubble on platinum microheater, *J. Appl. Phys*. 102 (2007) 034903.

[15] R. Siegel and E. G. Keshock, Effects of reduced gravity on nucleate boiling bubble dynamics in saturated water, *AIChE J*. 10 (1964) 509-517.

[16] G. Son, V. K. Dhir and N. Ramanujapu, Dynamics and heat transfer associated with a single bubble during nucleate boiling on a horizontal surface. *J. Heat Transfer* 121 (1999) 623-631.

[17] K. N. Rainey, K.N, S. M. You and S. Lee, Effect of pressure, subcooling and dissolved gas on pool boiling heat transfer from microporous, square, pin-finned surfaces in FC-72, Int. *J. Heat Mass Transfer* 46 (2003) 23-35.

[18] Y. Qi and J. F. Klausner, Heterogeneous nucleation with artificial cavities. *Proc. ASME Summer Heat Transfer Conf.* (2005).

[19] R. Cole, Bubble frequencies and departure volumes at subatmospheric pressures. *AIChE J*. 13 (1967) 779-783.

[20] H. J. Ivey, Relationships between bubble frequency, departure diameter and rise velocity in nucleate boiling, *Int. J. Heat Mass Transfer* 10 (1967) 1023-1040.

[21] P. W. McFadden and P. Grassman, The relation between bubble frequency and diameter during pool boiling, *Int. J. Heat Mass Transfer* 5 (1962) 169-173.

[22] T. H. K. Frederking and D. J. Daniels, The relation between bubble diameter and frequency of removal from a sphere during film boiling, *J. Heat Transfer* 88 (1966) 87-93.

Young Soo Chang received his B.S., M.S., and Ph.D. degrees from Seoul National University in 1991, 1993, and 1997, respectively. Dr. Chang is currently a principal research scientist at Korea Institute of Science and Technology in Seoul, Korea. His research interests include boiling heat transfer and refrigeration.

Kwang-Hun Jeong received his B.S. degree from Pusan National University in 2005 and his M.S. degree from Seoul National University in 2007. He currently works as an engineer in Doosan Heavy Industry.

Heon Ju Lee received his B.S. degree from Korea University in 2001 and his M.S. degree from Texas A & M University in 2003. He is currently on leave from his job at the Korea Institute of Science and Technology in Seoul, and is doing his Ph.D. program at MIT. His research interests are design and fabrication of MEMS.

Ho-Young Kim received his B.S. degree from Seoul National University in 1994, and his M.S. and Ph.D. degrees from MIT in 1996 and 1999, respectively. He is currently an associate professor of Mechanical Engineering in Seoul National University, Seoul, Korea. His research interests include microscale and biological fluid mechanics.